

# Transient helix formation in charged semiflexible polymers without confinement effects.

Debarshi Mitra<sup>1</sup>, Apratim Chatterji<sup>1,2\*</sup>

<sup>1</sup> *Dept. of Physics, IISER-Pune, Dr. Homi Bhaba Road, Pune-411008, India.*

<sup>2</sup> *Center for Energy Science, IISER-Pune, Dr. Homi Bhaba Road, Pune-411008, India.*

(Dated: December 28, 2021)

Switching on generic interactions e.g. the Coulomb potential or other long ranged spherically symmetric repulsive interactions between monomers of bead-spring model of a semi-flexible polymer induce instabilities in a semiflexible polymer chain to form transient helical structures. Our proposed mechanism could explain the spontaneous emergence of helical order in stiff (bio-) polymers as a chain gets charged from a neutral state. But since the obtained helical structures dissolve away with time, hydrogen bonding (or other additional mechanisms), would be required to form stabilized helical structures as observed in nature (such as in biological macro-molecules). The emergence of the helix is independent of the molecular details of the monomer constituent. The key factors which control the emergence of the helical structure is the persistence length and the charge density. We have avoided using torsional potentials to obtain the transient helical structures. Moreover, we can drive the semiflexible polymer to form helices in a recurring manner by periodically increasing and decreasing the effective charge of the monomers. If the two polymer ends are tethered to two surfaces separated by a distance equal to the contour length of the polymeric chain, which could be in the range  $10nm-\mu$ , the life time of the helical structures formed is increased.

## I. INTRODUCTION

Creating emergent structures through intelligent engineering of physical interactions between macro-molecules is a versatile method to self-assemble or self-organize structures with a target morphology. A particular macro-molecular morphology of great interest across disciplines is the helix, as it is a recurring motif across chemistry, biology[1–3] and physics [4–9]. Forging helical structures at the  $nm$  to  $10\mu$  length scales remain challenging, though helical springs are ubiquitous in NEMS/MEMS devices[10, 11], piezoelectric devices[12] and helical micro-swimmers[13–16] are used for micro-rheology. These helices are produced primarily by various “bottom up approaches”, e.g. vapour deposition which is dependent on the detailed interactions of the constituent atoms/ molecules, or alternatively using helical templates[17–23]. Helices can also emerge due to suitable confinement effects [24, 25]. It would be of interest to devise alternate strategies to obtain spontaneously formed helical architectures at  $nm-\mu$  length scales using physical forces by approaches which remain independent of chemical details of the monomer constituent.

There have been previous reports of extremely short lived helix formation in polymers in bad solvents undergoing collapse due to hydrophobic forces [6] which act at  $nm$  length scales. Others have observed helices on optimally packing tubular filaments at particular ratios of pitch and radius [4]. But in a more detailed paper, the authors comment that compaction of a chain of spheres gives very different results from compaction of a tube [1]. This is because the tube can be considered as a compact

object made up of discs which has very different symmetry properties in terms of interaction potentials compared to those acting between spherical beads, say, of a polymeric chain. Another study shows that the ground state of a self attracting chain shows a variety of structural motifs including the helix, depending on the nature of the stiffness present in the chain (energetic or entropic) [26]. Our study reports the self-emergence of free standing helical structures using the most generic of repulsive potentials such as Coulomb repulsion which could have influence in understanding emergence of such structures at  $nm-\mu$  length scales, in a variety of situations within the living cell or outside.

Here we show emergent structures with transient helical order in a free standing (unconfined) bead spring model of a semiflexible polymeric chain using generic interactions. Our computer simulations show that helical structures can be obtained by inducing instabilities with either Coulomb interactions or other long ranged power law repulsive interactions between the monomers if we start out from an initial configuration where the uncharged polymer chain is straight for a polymer chain whose persistence length is lesser than the contour length. At time  $t = 0$  if a neutral polymer becomes charged, the chain adopts a helical configuration before the helical structure dissolves to adopt a stretched linear configuration at long times due to long ranged repulsion. We also show that a stiff polymer chain in thermal equilibrium with its bath can also result in a helical conformation if repulsive Coulomb interactions between the monomers is switched on. A helical structure may also be obtained if a semi-flexible polymer chain, with persistence length  $\ell_p < N_c$  where  $N_c$  : the contour length) is pulled at both ends by a constant force, and released just as the repulsive Coulomb interaction is switched on between the monomers. Experimentally this may be accomplished by

---

\* apratim@iiserpune.ac.in

pulling the polymer chain with an AFM tip [27, 28] and the charges may be induced by changing the pH of the solution, [29–33].

Note that in all of the above we obtain transient helices without the use of torsion inducing potentials or hydrogen-bond mimicking potentials acting between monomers. In this paper, we also show how thermal fluctuations play an important role in the the formation of helical structures. In addition, we induce time dependent potentials where the charge of a semi-flexible polymer varies with time (say as pH changes with time) [34, 35]. As a consequence, helices are formed periodically in phase with the driving.

The manuscript is organized as follows. The following section describes the model of a semi-flexible polymer dressed with additional long range interactions which leads to helix formation. The additional interactions have the form  $\sim 1/r$ , or  $\sim 1/r^3$ . This implies that there is no screening of Coulomb charges, when we describe helix formation starting out from a straight line initial condition or of a stiff polymer in thermal equilibrium or from a stretched condition due to force applied to the end monomers. Next we discuss the mechanism of helix formation starting out from a straight line initial condition (for simplicity) with  $1/r$  (Case A) and  $1/r^3$  (Case B). At the end we discuss the range of values of semi-flexibility energies/spring constants/strength of Coulomb forces for which we obtain helices. We do this by plotting a suitable state-diagram. We finally conclude with Discussions and future outlook.

## II. MODEL

We use the bead spring model of a polymer for our simulations. The model polymer could be a real polymer, or it can be string of colloids stitched together to form a semi-flexible polymeric chain as described in [36, 37]. Thereby, the monomer size and the number of beads  $N$  in the chain determine the length scale of helical configurations formed. The unit of length in our study is  $a$ , where  $a = 1$  is the equilibrium length of the harmonic-springs between two adjacent monomers with energy  $u_H = \kappa(r - a)^2$  between adjacent monomers;  $r$  is the distance between the monomers. The spring constant  $\kappa$  is  $20k_B T/a^2$  for Case A, which has repulsive Coulomb interactions  $u_c = \epsilon_c(a/r)$  acting between all monomer pairs of the chain. The parameter  $\epsilon_c = 87.27k_B T$  is the measure of the Coulomb energy when a pair of charges are at a distance  $a$  from each other. Case B uses  $\kappa = 10k_B T/a^2$ , along with the additional interaction  $u_d$  between all the monomers of the chain. The form of the potential  $u_d$  is  $u_d = \epsilon_d(a/r)^3$  with  $\epsilon_d = 107.70k_B T$  with cutoff at  $r_c = 4a$ . Diameter of each monomer is  $\sigma = 0.727a$ , and excluded volume (EV) of monomers are modeled by the WCA (Weeks Chandler Anderson) potential. This choice corresponds to the good solvent condition.

The polymeric chain is semi-flexible; the corresponding

bending energy  $u_b$  is  $u_b = \epsilon_b \cos(\theta)$ , where  $\theta$  is the angle between vectors  $(-\mathbf{r}_i, \mathbf{r}_{i+1})$ . The vector  $\mathbf{r}_i$  is the vector joining monomer  $i - 1$  to its neighbouring monomer  $i$  along the chain contour. The thermal energy  $k_B T = 1$  sets the energy unit. We performed Brownian dynamics simulations where the friction constant is  $\zeta$ , and the unit of time  $\tau$  is set by  $\tau = a^2 \zeta / k_B T$ , the time taken for a isolated monomer particle to diffuse a distance of  $a$ . If we set  $\zeta = 1$  such that  $\tau = 1$ , since  $k_B T$  and  $a$  are already chosen to be one, the over-damped stochastic Brownian dynamics equation is integrated with time step  $dt = 0.0001\tau$ .

Unless clarified otherwise, we mostly observe the polymer dynamics by starting out from the same straight line initial condition for the above mentioned cases (A) and (B): a linear polymer chain of 49 monomers is placed along the  $y$  axis with adjacent monomers at a distance of  $a$  from each other. The fluctuation dissipation theorem determines the magnitude of the random force on each particle for all cases. For studies with cases (A) and (B), we choose  $\epsilon_b = 10k_B T$  (corresponding to the persistence length  $\ell_p = 11a$ , as calculated by simulations) and  $80k_B T$ , respectively. A large difference in the values of  $\epsilon_b$  was chosen to demonstrate that helix formation is robust for a range of parameter values. We use box-size  $\gg 50a$  for a chain with 49 beads, such that periodic boundary conditions are never invoked. Hence we do not use Ewald technique to calculate Coulomb interactions as self interactions with periodic images of the monomers are irrelevant. Moreover, no counterions were considered for our simulations, so the charges are not screened.

Subsequently, we study transient helix formation of chains in thermal equilibrium, *viz.*, we establish that a semiflexible polymer with 60 monomers in the chain and with persistence length  $\ell_p$  greater than the contour length  $N_c = 60a$  and in thermal equilibrium with the bath, develops a local helical order once the repulsive Coulomb interactions ( $\epsilon_c = 87.27k_B T$ ) between the monomers is switched on. The spring constant  $\kappa = 200k_B T/a^2$ . Furthermore, if a semi-flexible polymer, with 60 monomers in the chain but with  $\ell_p < 60a$ , is stretched by applying a constant force at both ends by a constant force  $20k_B T/a$  and then released, and simultaneously the repulsive Coulomb interaction ( $\epsilon_c = 87.27k_B T$ ) is switched on between the monomers, then the polymer again develops a transient helical order.

From the experimental perspective, it would be more instructive to specify the  $\ell_p$  of a polymer rather than specify the the simulation parameter  $\epsilon_b$ , which we tune to fix  $\ell_p$ . To that end, we calculate the relation between  $\epsilon_b$  and  $\ell_p$  for small angular deviations of bond-angles from angle  $\pi$ . The calculation details are given in the appendix. The relation between angle  $\alpha$  (as shown in the Fig.14 of appendix) and  $\epsilon_b$  is given by,

$$(\epsilon'_b - 1)/\epsilon'_b = \cos \alpha \quad (1)$$

where  $\epsilon'_b = \epsilon_b/k_B T$  and  $\alpha = \pi - \theta$ . From polymer physics [38], we know that for WLC (worm like chain) model, for

the small angles of bends, the persistence length  $\ell_p$  is given by  $\ell_p = 2a/\alpha^2$ . Thereby,

$$\ell_p \approx a\epsilon_b/k_B T \quad (2)$$

Thus  $\ell_p$  increases linearly with  $\epsilon_b$ . As an example, a polymer with bending energy  $\epsilon_b = 10k_B T$  will have persistence length  $\ell_p \approx 10a$  as per the above equation. This matches with the earlier mentioned value of  $\ell_p = 11a$ , where we explicitly calculated the  $\ell_p = 11a$  from the decay of the correlation function of the end-to-end vector for a semi-flexible polymer (with  $u_c$  kept fixed at 0). At higher values of  $\epsilon_b$ , the Eqn.2 will be more accurate.

### III. RESULTS AND ANALYSIS:

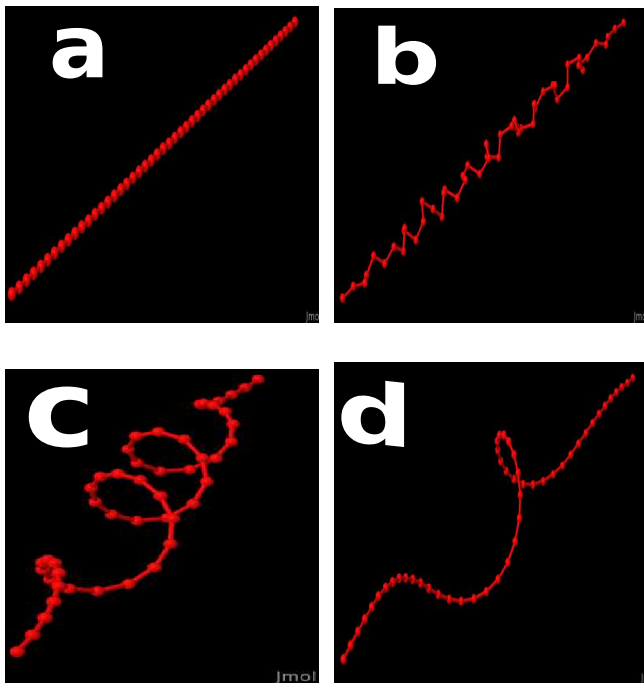


FIG. 1. Figures 1(a-d) shows various stages of the helical instability for a semi-flexible polymeric chain starting from the straight initial configuration with potential  $u_d$ : case B. The snapshots are (a) for the straight line initial configuration at time  $t = 0$  with 49 monomers (b) the configuration at time  $t = 3.3 \times 10^{-2}\tau$  ( $H2 = 0.23$ ,  $H4 = 0.006$ ) (c) the configuration at a subsequent time  $t = \tau$ , when the helix is formed ( $H2 = 0.81$ ,  $H4 = 0.43$ ) (d) configuration showing the unwinding of the helix at time  $t = 5\tau$  ( $H2 = 0.65$ ,  $H4 = 0.29$ ). The corresponding snapshots with potential  $u_c$  (Case A) are in the supplementary.

In Figure 1 we show representative snapshots from various stages of transient helix formation for a polymer with interaction energies corresponding to case-B starting out from a straight initial condition. As the bead-spring model of polymer chain starts out from the straight line

initial configuration (refer Fig.1a), the thermal forces randomly displace the monomers from their initial positions. Furthermore, strong repulsive forces arising from  $u_d$  act along the line joining the centers of monomers make the monomers move away from each other, accentuating the angle between adjacent bonds and consequently the polymer forms a locally kinked structure as shown in Fig.1b which is penalized by the bending energy term. Thereby, the helical conformation of the polymer emerges at sections of the chain at a time  $t \sim \tau$  to locally relax the high bending energy costs due to kinks as seen in Fig.1c. But it dissolves away at times  $t \gg \tau$  (refer Fig.1d). The unit of time of the problem is chosen as  $\tau = (\zeta a^2/k_B T)$ , the time taken for a isolated monomer particle to diffuse a distance of  $a$ .

Random fluctuations due to  $k_B T$  displace the monomers just after time  $t = 0$ , which in turn leads to the development of the helical order, and thereby  $k_B T$  plays a crucial role though  $\epsilon_c, \epsilon_d$  and  $\kappa, \epsilon_b$  are all  $\gg k_B T$ . A perfectly straight polymer configuration at  $T = 0$  stretches out but never gets to form helices as all the forces between monomers act along the line joining the centers. Movies S1, S2 in the Supplementary section helps the reader to visualize the instability which results in helix formation for Case-A & Case-B, respectively. Movie S3 is for Case B with potential  $u_d$  with  $k_B T = 0$ , and as a consequence the polymer does not form transient helical structures.

We quantify the emergence of helicity as a function of time by calculating and plotting two quantities in Fig.2(a,b) and Fig. 2(c,d) for cases A and B, respectively, viz., the global order parameter  $H4$  and the local order parameter  $H2$  where,

$$H4 = \frac{1}{N-2} \left( \sum_{i=2}^{i=N-1} \mathbf{u}_i \right)^2; H2 = \frac{1}{N-3} \left( \sum_{i=2}^{i=N-2} \mathbf{u}_i \cdot \mathbf{u}_{i+1} \right) \quad (3)$$

where  $\mathbf{u}_i$  is the unit vector of  $\mathbf{U}_i = \mathbf{r}_i \times \mathbf{r}_{i+1}$ . A compact tightly wound perfect helix in the continuum picture with infinitesimal  $\mathbf{r}_i, \mathbf{r}_{i+1}$  vectors will have vectors  $\mathbf{u}_i$  pointing along the helix axis, and hence  $H4$  will have a value of  $\approx 1$ . However, if one obtains a helical structure where half of the chain is right handed, and the rest of it is left-handed,  $H4$  will be zero. Hence, we need the other parameter  $H2$  to identify local helical order [6, 39]. A simple semi-flexible polymer chain ( $u_c = 0$  &  $u_d = 0$ ) shows  $H2, H4$  values  $\approx 0$  (or negative values of  $H2$ ) as expected for a chain locally bent due to thermal fluctuations. But the polymer chains with additional interactions  $u_c$  or  $u_d$  lead to the formation of transient helices with distinctly non-zero positive values of  $H2, H4$ . The time taken for the helix to form is  $\approx 0.5\tau$ . Note that  $H2$  is equal to  $\langle \cos(\phi) \rangle$  where  $\phi$  denotes the torsion angle, i.e. the angle between the planes formed by adjacent pair of the monomer-triplets along the length of the chain; the average is taken over the cosine of the various torsion angles formed along the length of the chain.

We also investigated the emergence of helices in chains

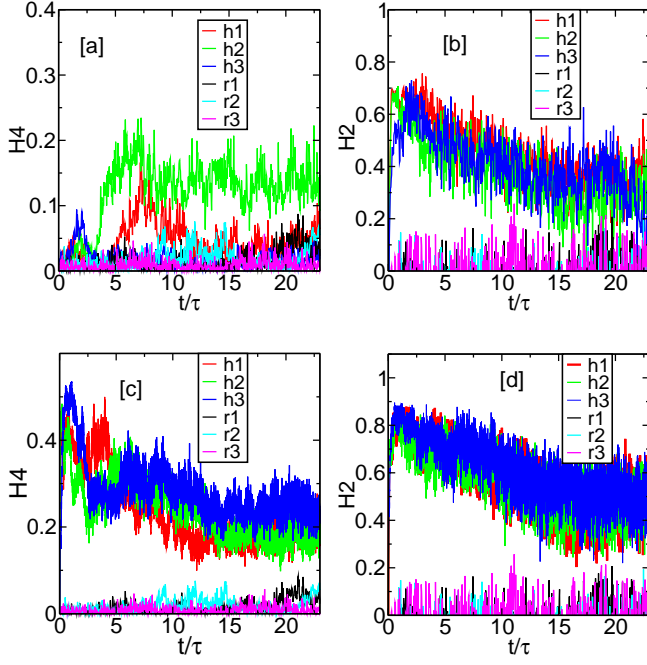


FIG. 2. Subfigures (a),(b) shows  $H4$  and  $H2$  versus time  $t$  of a semi-flexible polymer chain of 49 monomers for three independent runs denoted by  $h1, h2$  and  $h3$  starting out from a straight initial configuration of the chain. Potential  $u_c$  acts between all monomers pairs. The interaction strengths correspond to Case A. For comparison, we also show  $H4, H2$  values obtained for a semi-flexible polymer chain of 49 monomers with  $u_c = 0$  starting from the same initial condition; these are denoted by  $r1, r2$  and  $r3$ . Subplots (c),(d) shows  $H4$  and  $H2$  versus time of the semi-flexible polymer chain of 49 monomers for three independent runs denoted by  $h1, h2$  and  $h3$ , such that potential  $u_d$  acts between all monomer pairs; the interaction energies correspond to case B. The initial configuration is a straight chain along y axis. The three independent runs for a chain of same length with  $u_d = 0$  are denoted by  $r1, r2$  and  $r3$ . Note that  $H2$  is equal to average of the values of  $\cos(\phi_i)$ ;  $\phi_i$  are the torsion angles subtended along the chain contour. In each figure, data for  $H2, H4$  is plotted every 1000 iterations, i.e. every  $0.1\tau$ .

of  $N = 25$  and  $N = 100$  monomers, respectively (refer supplementary data). A chain of 100 monomers has approximately 5 helical segments and thereby has relatively lower values of  $H4$  in some of the independent runs, since different segments can form helices of opposing handedness. But the values of  $H2$  obtained for  $N = 25$  or  $N = 100$  are comparable to that obtained for the  $N = 49$  polymer chain at time  $t = 2\tau$ . Thus we establish that we indeed get helical conformations in our model semi-flexible polymer as long as we have long-ranged repulsive interactions between the monomers.

Furthermore, to establish that the helix formation is not just a consequence of the special straight line initial condition, we calculate  $H2$  to establish the development of helical order in a semi-flexible polymer in thermal equi-

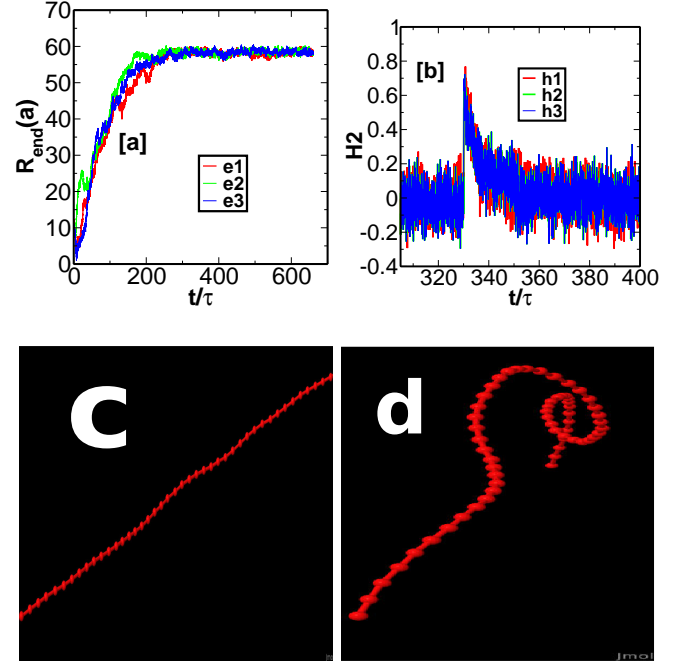


FIG. 3. Subfigure (a) shows the end to end distance  $R_{end}$  versus time for an uncharged, semiflexible polymer chain of 60 monomers having  $\epsilon_b = 400k_B T$  ( $\ell_p = 400a$ ) and  $\kappa = 200k_B T/a^2$  for three independent runs  $e1, e2$  and  $e3$ . Initially the monomers were placed randomly, and we conclude that  $R_{end}$  takes about  $200\tau$  to reach its equilibrium value. Subfigure (b) shows  $H2$  versus time for the 60 monomer polymer chain such that the repulsive Coulomb interaction ( $\epsilon_c = 87.27k_B T$ ) is switched on at  $333.33\tau$ . This led to a increase in the value of  $H2$  which later decreases as the helical order dissolves away. The data for three independent runs are labelled as  $h1, h2$  and  $h3$ . Subfigure (c) shows the snapshot of the polymer configuration just before helix formation ( $H2 = -0.09, H4 = 0.008$ ). Subfigure (d) shows the snapshot of the conformation of the polymer which has helical order ( $H2 = 0.65, H4 = 0.09$ ).

librium. The Coulomb potential  $u_c$  and corresponding forces between monomer is switched on after ensuring that the polymer is in equilibrium. We choose a polymer whose persistence length greater than the contour length, place the monomers randomly and allow the polymer to relax and reach equilibrium such that the end to end vector fluctuates about an average value. Initially the end-to-end distance  $R_{end}$  increases as the bent polymer straightens itself. In Fig.3a we show  $R_{end}$  versus time  $t$  for the semiflexible polymer chain with 60 monomers, such that its length is  $60a$  and  $\ell_p = 400a$ . Data is shown for three independent runs,  $e1, e2$  and  $e3$ . We observe that it takes approximately  $200\tau$  for it to reach the equilibrium value. For Fig.3b we again take the same semi-flexible polymer with 60 monomers and switch on the repulsive Coulomb interaction ( $u_c$  with  $\epsilon_c = 87.27k_B T$ ) between the monomers at  $333.33\tau$ . We observe that there is a significant increase in the value of  $H2$  immediately after  $t = 333.33\tau$ . The  $H2$  value then gradually decreases, in-



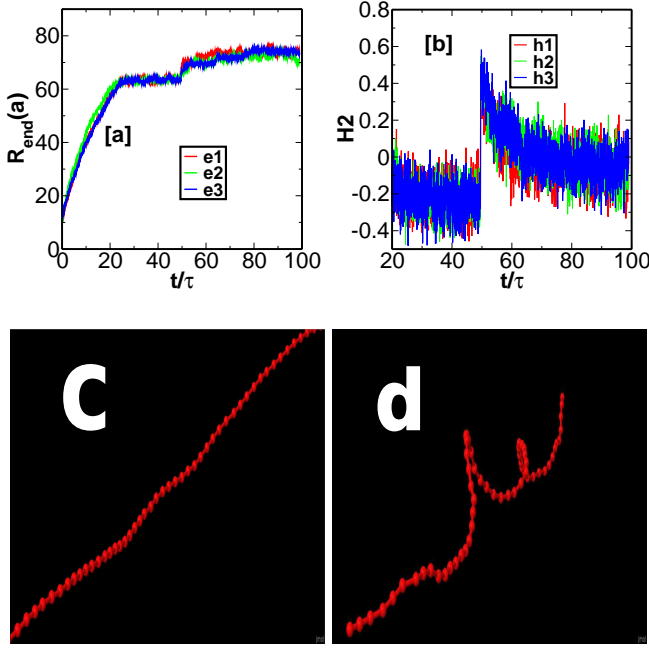


FIG. 4. Subfigure (a) shows the end to end distance  $R_{end}$  versus time  $t$  for a polymer chain of 60 monomers,  $\epsilon_b = 30k_B T$  ( $\ell \approx 30a$ ) and  $\kappa = 200k_B T/a^2$ , where the end monomers are pulled outwards by the application of a constant force of  $20k_B T/a$  in opposite directions. data is presented for 3 independent runs  $e1, e2$  and  $e3$ . Note that the Coulomb repulsion ( $\epsilon_c = 87.27k_B T$ ) between monomers was switched on at  $50\tau$  and the stretching force was set to 0, simultaneously. Subfigure (b) shows  $H2$  versus time for the polymer chains having the same parameters values in (a). We once again see transient helix formation and its dissolution for three independent runs,  $h1, h2$  and  $h3$ . Subfigure (c) shows the snapshot of the polymer configuration just before the Coulomb interaction is switched on ( $H2 = -0.26, H4 = 0.012$ ). Subfigure (d) shows the snapshot of the helical conformation of the polymer ( $H2 = 0.58, H4 = 0.10$ )

indicating that a transient helical structure dissolves away. Fig 3c and Fig3d show the snapshots of the helical conformation just before and after  $u_c$  was switched on.

Suppose we have a polymer chain of length  $60a$  with  $\ell_p = 30a$  in thermal equilibrium, such that the persistence length is lower than the contour length. If we switch on  $u_c$ , we do not get any distinct helical order. However, if we stretch the polymer (say by a AFM-atomic force microscopy tip) and then switch on  $u_c$ , we again see emergence of a transient helical order. A semi-flexible chain can be stretched by applying a suitable value of a constant force ( $\vec{F}_{\pm} = \pm(20k_B T/a) \hat{y}$ ) at both ends such that its end to end distance  $R_{end}$  becomes  $\approx 60a$ . We then allow the chain to explore different equilibrium conformations in the presence of the fixed stretching force acting on the end monomers.

Then the tension is released by switching off the force applied to the end monomers and simultaneously the re-

pulsive Coulomb interaction ( $u_c$  with  $\epsilon_c = 87.27k_B T$ ) is switched on between the monomers. In such a *in-silico* experiment, we do see the emergence of helical order by the measurement of  $H2$ . The relevant data is shown in Fig.4. In Fig.4a we show the evolution of  $R_{end}$  under the application of equal and opposite forces acting on the end monomers of the chain. The mean  $R_{end}$  reaches a mean value greater than the contour length in three independent runs within time  $20\tau$ . At  $50\tau$  there is an increase in the end to end distance because at this point the stretching force is released and the repulsive Coulomb interaction (with  $\epsilon_c = 87.27k_B T$ ) is switched on. In Fig.4b we observe that there is a corresponding significant increase in the value of  $H2$  which gradually decreases indicating that a transient helical structure was formed, which dissolves away. Fig.4c and Fig.4d show the snapshots of the helical conformation just before and soon after the repulsive Coulomb interaction was switched on between the monomers.

But what is the physics of helix formation in the semi-flexible polymer chains in the presence of spherically symmetric repulsive potentials  $u_c$  or  $u_d$ ? What role does temperature play? For the remainder of the manuscript, for simplicity, we report the dynamics of a polymer chain in a thermal bath starting out from a straight initial linear conformation.

To develop a detailed understanding of the mechanism of helix formation we note that just after time  $t = 0$  the thermal kicks displace the monomers from a straight line initial condition. Thereafter, the magnitude of this random displacements gets accentuated by the repulsive  $u_c$  (or  $u_d$ ) acting along the line joining the monomer centers, accompanied by an increase in the distances between monomers. This results in the lowering of the Coulomb energy per particle  $U_c$  (or  $U_d$ ). However, sharp local kinks get created as is seen in Fig.1b and also results in increase of the contour length of the polymer. To release the bending energy due to sharp kinks, the kinked structure evolves to a structure with local helicity at different segments of the chain. We follow the values of the various contributions to the total energy  $U_{tot}$  as a function of time in Fig.5 to understand the development of structure of the polymer. Increase in the bond energy per spring,  $U_H$  with time  $t/\tau$  indicates a corresponding stretching of bonds between adjacent monomers: we have independently checked that the bonds stretch and do not get compressed. Similarly an increase in the value of semi-flexible energy per triplet of monomers,  $U_b$ , would be indicative of sharp bends along the contour of the polymer chain.

We now discuss this in more detail. Just after time  $t = 0$  the chain remains nearly straight with the bending energy per each bend nearly equal to  $-\epsilon_b \cos \theta = -10k_B T$  since  $\cos \theta \approx -1$  (case A). However, for time  $t/\tau < 0.003$ , the  $U_H$  increases slowly from value 0 due to random shifts in the monomer positions because of thermal fluctuations. But this increase is not discernible in the plots of the energy contributions versus time in Fig.5, but can be

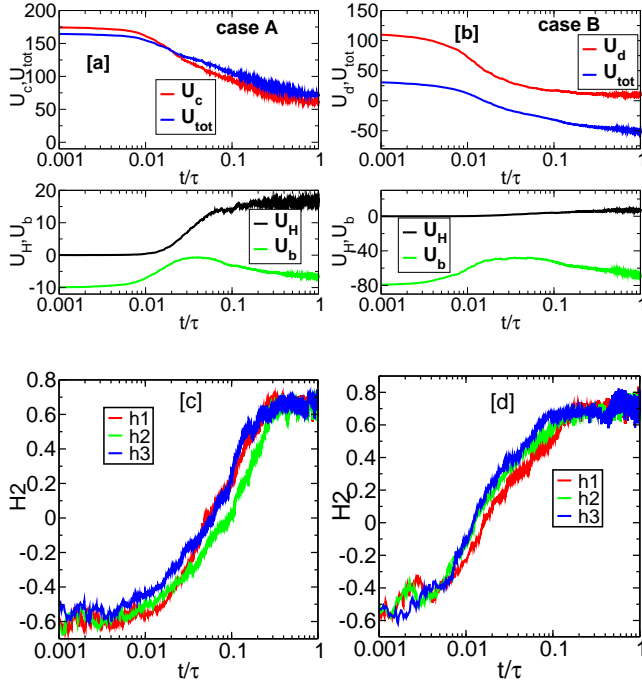


FIG. 5. Subplots (a) and (b), corresponding to case A and case B, shows energies  $U_H$ ,  $U_b$ ,  $U_{tot}$  and  $U_c$  or  $U_d$ , respectively, where  $U_{tot}$  denotes the total energy per monomer and is the sum of  $U_H$ ,  $U_b$  and  $U_c$  or  $U_d$ . The x-axis shows  $t/\tau$  for relatively short times, i.e.  $t < \tau$ . Subfigures (c) and (d) show  $H2 = \langle \cos \phi_i \rangle$  versus  $t/\tau$  for three independent runs  $h1$ ,  $h2$  and  $h3$  with  $u_c$  and  $u_d$  acting between the monomers, respectively. The angle  $\phi_i$  also denotes the dihedral angle between the two planes formed by the monomers  $(i, i+1, i+2)$  and  $(i+1, i+2, i+3)$ , respectively. The index  $i$  represents any monomer along the chain. The cosine of the angle  $\phi_i$  was averaged along the length of the chain for all possible values of  $i$  to yield  $H2 = \langle \cos \phi_i \rangle$  at time  $t$ .

seen in the log-log plot of energy versus time given in the supplementary section. Thereafter, formation of sharp bends/kinks resulting from the motion of monomers due to repulsive Coulomb forces (or from  $u_d$ ) leads to the rapid increase of both  $U_H$  and  $U_b$  which is seen in 5(a,b) at times  $t/\tau > 0.01$ . This is accompanied by a decrease in the Coulomb energy per monomer  $U_c$  (and  $U_d$ ), again refer Figs.5(a,b).

Following the rapid increase in  $U_b$  from time  $0.01 < t/\tau < 0.03$ , there is a sharp increase in forces trying to straighten the chain. The monomers still move apart from each other due to Coulomb repulsion, but simultaneously try to decrease the bending energy costs by radially spreading out the monomers locally in a manner such that the change in the bending angles along the chain contour becomes gradual. This dynamics can be deduced by observing the decrease of  $U_b$  after it reaches its peak at time  $t/\tau \approx 0.03$ . As a consequence of the local radial spreading out of the monomers, the chain develops helicity along the length of the chain, refer Figs.5(c,d).

Note that the motion of a segment would also be constrained by the motion of adjacent segments along the chain. Thus, different segments of the chain could thus develop clock wise or anti-clock wise helicity since the initial deviations from the straight line configuration were in random directions due to thermal fluctuations.

The evolution of a straight chain into helical structures can also be followed by looking at the average (along the length of the contour) of the average of the cosine of the torsion angles along the length of the chain (as given by  $H2$ ), as a function of time. This is plotted in Fig.5(c) and (d) for cases A and B, respectively. At time  $t = 0$ , when we have a straight chain, a plane between monomer triplets is undefined and so is the normal to the plane. But as soon as the monomers move due to thermal energy, planes can be defined using the positions of adjacent monomer-triads and outward normals  $\mathbf{u}_i$  to these planes can point in any direction but mostly normal to the  $y = 0$  plane. At slightly longer times (i.e. when the sharp kinks get formed), since all values of  $\cos(\phi)$  are possible, the average of  $\cos(\phi)$  along the chain quickly goes to zero with time  $t$  for all the three independent runs. However, as the chain develops helical order beyond time  $t/\tau > 0.05$ ,  $\langle \cos(\phi) \rangle$  reaches a values in the range  $0.4 - 0.6$ , corresponding to an angle of around  $\sim 60^\circ$ .

At times beyond  $t/\tau > 1$ , i.e. after the helix has already been formed, the value of  $u_H$  for the stretched springs starts fluctuating around an average value. However, uniform relatively uniform bends of a helical configuration are penalized by  $u_b$  and hence at times  $t > 2\tau$  the uniform helical structures start to gradually locally unwind leading to a gradual increase in the pitch (data given later) of the helical structure. This can be understood by looking at the evolution of energies  $U_c$ ,  $U_b$  and  $U_H$  with time in Fig.6(a,b) (case A) and in Fig.6(c,d) (case B). We also show  $U_{tot}$  which is the sum of  $U_c$ ,  $U_b$  and  $U_H$ . There is a slight decrease in  $U_c$  or  $U_d$  with time and the values of the bending energy  $U_b$  also show a steady but slow decrease with time.

The next figure, Fig.6 shows the long time behaviour of the  $U_c$ ,  $U_b$  ( $U_d$ ),  $U_H$  and  $U_{tot}$  as the helical conformations dissolve. From Fig.6b and Fig.6d it is evident that there is a crucial difference between Case A and Case B which arises from the difference in the rate of fall of the potential with increasing  $r$ . For Case A,  $U_c$  shows a decrease of about  $\sim 8k_B T$  with time, whereas  $U_d$  shows a decrease of about  $\sim 2.5k_B T$  over  $20\tau$ . Consequently the total energy per monomer,  $U_{tot}$  for the two cases also show a larger decrease for case A, as seen in Fig.6a and Fig.6c. This implies that the polymer chain in case A has a higher tendency to unwind and stretch itself out to a relatively more straight configuration due to the repulsive forces of  $u_c$  as compared to polymer with potential  $u_d$  of case B. This is in spite of the value of  $\epsilon_b$ , which is much higher for case B. This is consistent with the data of  $H2$  relaxation with time shown in Fig.2(b,d) and explains why  $H2$  for case B shows relatively higher values as compared to  $H2$  of case A at times  $t > 1$ .

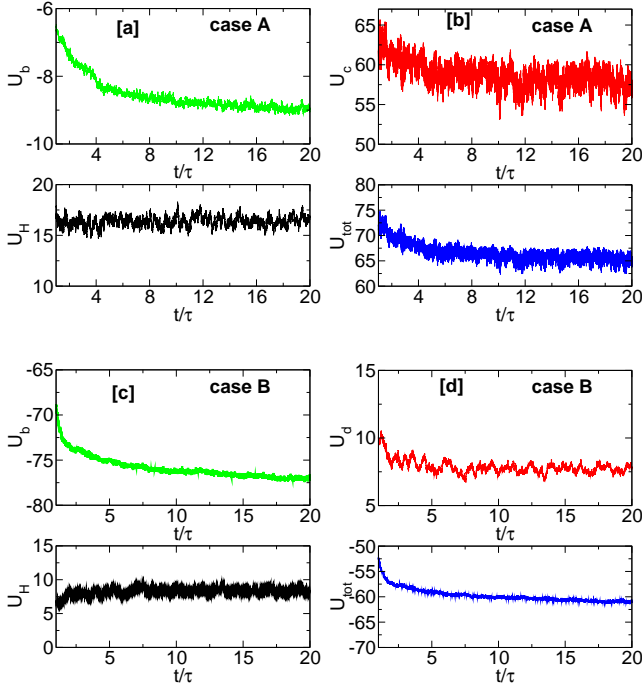


FIG. 6. Subplots (a) , (b), (c) and (d) show the same quantities as in Fig.5 (a,b) but over longer times  $t > \tau$  and the x-axis is shown in linear scale. The parameters are the same as mentioned previously in fig.5. Subplot (a) shows the values of spring energy  $U_H$  per monomer, and the bending energy  $U_b$ , per bend versus time  $t/\tau$  corresponding to case-A. Subplot (b) shows the values of repulsive potential energy  $U_c$ , and the total energy  $U_{tot}$ , per monomer versus time corresponding to Case A. Subplot (c) shows the values of spring energy  $U_H$ , and the bending energy  $U_b$ , per monomer versus time corresponding to Case B . Subplot (d) shows the values of repulsive potential energy  $U_d$ , and the total energy  $U_{tot}$ , per monomer versus time corresponding to case-B.

Thermal fluctuations provide the initial random forces which leads to the slight displacement of the monomers away from its initial straight line configuration which makes the linear configuration unstable. At temperature  $T = 0$ , the polymer starting from a initial straight configuration along  $\hat{y}$ , stretches out to reach its minimum energy configuration in presence of  $U_c$  but never forms helices as forces arising from  $u_c$  (or  $u_d$ ) and  $u_H$  act along the line joining the centres of the monomers (refer movie S3 in Supplementary section). At temperature  $T > 0$  and for time  $t/\tau > 0$ , the monomers move away from the straight line configuration, which leads to force components along the  $\hat{x}$  and the  $\hat{z}$  directions from  $u_c$  and  $u_b$ , and results in the emergence of helical conformations when  $U_c \neq 0$  (or  $U_d \neq 0$ ). To establish these conclusions, we ran a simulations to calculate  $H2$  and  $H4$  at temperature  $T = 0$ , however, starting from a uniformly curved initial condition such that the chain forms an arc in  $x - y - z$  plane (refer Fig 7c). Such an initial conformation again leads to helical instabilities due to forces

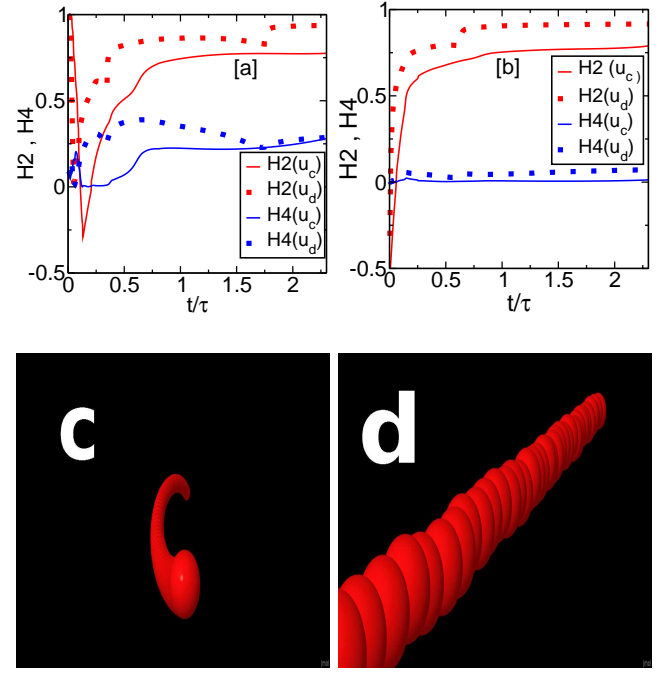


FIG. 7. Subplot (a) shows  $H4$  and  $H2$  versus time for a polymer chain corresponding to  $u_c$  and  $u_d$ , respectively, at  $k_B T = 0$  starting from a curved initial conformation. Subplot (b) shows  $H4$  and  $H2$  versus time for a polymer chain corresponding to  $u_c$  and  $u_d$  acting between the monomer pairs, respectively at  $k_B T = 0$  starting from an initial condition in which the polymer aligned with  $\hat{y}$  has small random displacements along  $\hat{x}$  and  $\hat{z}$ . The starting configurations for (a) and (b) are given in subfigures (c) and (d), respectively.

along the  $x$  axis and the  $z$  axes and therefore results in helices (as seen in data of Fig.7a). Alternatively, starting from an initial configuration of a relatively straight polymer chain along the  $y$ - axis but with small random displacements of all monomers along  $x$  and  $z$  coordinates maintaining temperature  $k_B T = 0$  (refer Fig. 7d), we still obtain a helical conformation of the polymer as seen in the data of Fig.7. Details of the initial conditions are described in the Supplementary section.

Thus the role of temperature is to introduce deviations from the straight linear conformation, and this triggers the helical instability. Since the local helical instabilities are triggered by random fluctuations at finite  $k_B T$ , we do not have any control on the handedness of the chain at different segments of the chain. Furthermore, if a single or a couple of monomers are slightly displaced from a straight line configuration at  $T = 0$ , then the semi-flexibility drives the chain to become straight and it then stretches out along a straight line to reach its energy minimum configuration. Thereby it does not form a helix provided the magnitude of the displacement of the monomers from the straight linear conformation of the chain is lesser than a certain value. To substantiate the same we ran the simulations at  $k_B T = 0$  for a poly-

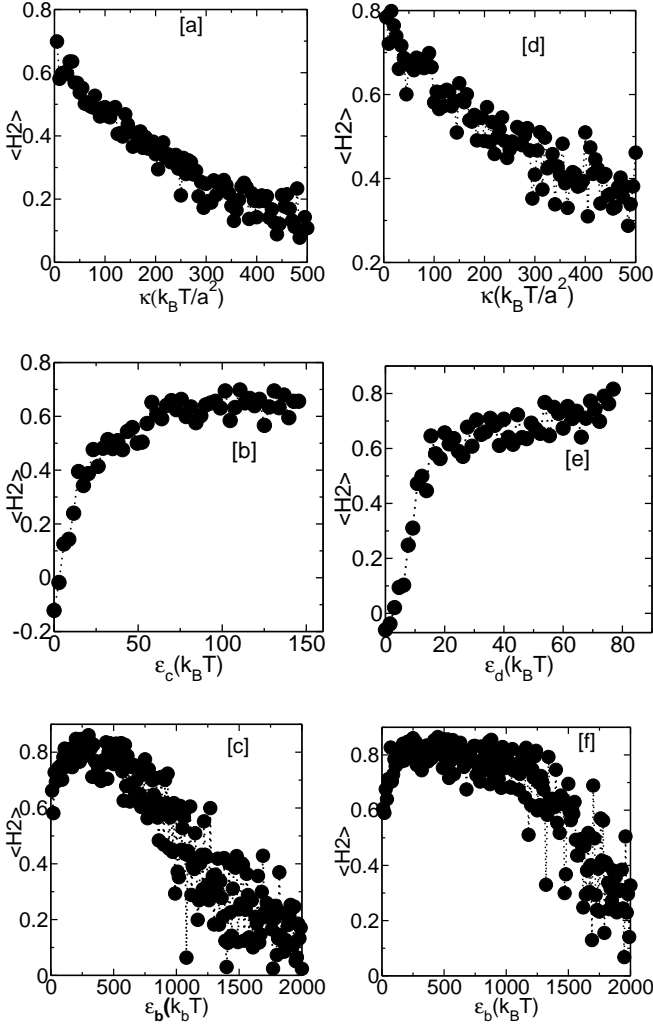


FIG. 8. Semiflexible polymer with  $\kappa = 20k_B T/a^2$ ,  $\epsilon_c = 87.27k_B T$  &  $\epsilon_b = 10k_B T$  corresponding to case-A : (a),(b),(c) show change in time averaged value of  $\langle H2 \rangle$  with increase of  $\kappa$ ,  $\epsilon_c$ ,  $\epsilon_b$ , respectively. We change one parameter at a time keeping the other two parameters fixed. Semiflexible polymer with  $\kappa = 10k_B T/a^2$ ,  $\epsilon_d = 107.70k_B T$  &  $\epsilon_b = 80k_B T$  corresponding to case-B: (d),(e),(f) show change in time averaged value of  $\langle H2 \rangle$  with increase of  $\kappa$ ,  $\epsilon_d$ ,  $\epsilon_b$ , respectively, keeping two other parameters fixed. The time averaged  $\langle H2 \rangle$  was calculated over  $0.66\tau$ , starting from  $t = 0.66\tau$  to  $t = 1.32\tau$ .

mer chain of 49 monomers with  $u_c$  acting between all monomer pairs and other parameters pertaining to that of Case A. The simulations reveal that if the magnitude of the displacements from the straight linear conformation of the arbitrarily chosen monomers (42nd and 13th in our case) is lesser than  $0.0028a$  we do not obtain helices. For displacements of magnitudes greater or equal to that of  $0.0028a$  we obtain helices. We show  $H2$  and  $H4$  versus time for a polymer chain of 49 monomers at  $k_B T = 0$ , with the 13th and the 42nd monomer displaced from the straight linear conformation by  $0.0028a$

and other parameters pertaining to that of Case A (refer Supplementary).

For a different choice of displaced monomers, the minimum displacement essential for helix formation will change. This is because the monomers of the polymer chain experience different net repulsive forces depending on their relative positions with respect to other monomers. It is also to be noted that for higher values of semi-flexibility a larger magnitude of the displacement of the monomers from the straight linear conformation would be required for the repulsive interactions to overcome semi-flexibility. We emphasize that the helical configuration at  $T > 0$  is not a energy minimum state but a configuration that the polymer accesses in its kinetic pathway to its (free) energy minimum state which is a stretched straight configuration(s) of monomers with local bends depending on the relative strengths of  $u_b$  and  $k_B T$ .

At non-zero  $k_B T$ , if the soft spring ( $\kappa = 10k_B T/a^2$  and  $\kappa = 20k_B T/a^2$  for cases A and B, respectively) joining the monomers becomes too stiff then the the position of monomers do not time-evolve to form a helix in response to forces arising from  $u_c$  and  $u_d$ . For high values of  $\kappa$ , stiff springs do not permit monomers to radially stretch out locally, thus preventing helix formation. We refer the reader to Figs.8 (a,d) which shows the decreasing values of the  $\langle H2 \rangle$  order parameter with increasing values of  $\kappa$ . The angular brackets in  $\langle H2 \rangle$  denote the average value of  $H2$  calculated using data collected between  $0.66\tau$  to  $1.32\tau$ . On the other hand, increase in the value of  $\epsilon_c$  in  $u_c$  (or  $\epsilon_d$  in  $u_d$ ) increases propensity of helix formation as observed in the increase in the value of  $\langle H2 \rangle$  with  $\epsilon_c$  (or  $\epsilon_d$ ) in Figs.8(b,e). For values of  $\epsilon_c > 50k_B T$  and  $\epsilon_d > 20k_B T$ ,  $\langle H2 \rangle$  nearly saturates to values of  $0.75$ . There is no helix formation when  $u_c, u_d = 0$ .

High values of  $\epsilon_b$  in the expression for  $u_b$  hinder the formation of sharp kinks which subsequently stretch out radially to give rise to the helical structures, thereby, suppresses the instability: refer Figs.8(c,f) corresponding to cases with potentials  $u_c, u_d$ . We get finite values of  $H2$  even when  $\epsilon_b = 0$ , as a charged polymer chain with the same sign of charge on the monomers behaves like a semi-flexible chain [40–43]. Hence, an increase in the values of  $\epsilon_b$  from zero leads to an initial increase of  $\langle H2 \rangle$  as increased bending energy costs help in radially spreading out the polymer as it leads to reduction of bending energy. Thereby,  $\langle H2 \rangle$  reaches a peak value of  $0.9$  at intermediate  $\epsilon_b$  values. But thereafter,  $\langle H2 \rangle$  starts decreasing with further increase of  $\epsilon_b$  as reasoned earlier.

Thus only in a certain range of these interactions of  $u_c$  (or  $u_d$ ) and  $u_b$  do we obtain well formed helices. This is further illustrated by the two state diagrams shown in Figs.9 which map out the average values of  $H2$  for various combinations of the values of  $\epsilon_c$  (or  $\epsilon_d$ ) and  $\epsilon_b$ . To obtain the colormaps shown in Figs.9(left) and 9(right),  $\kappa$  was fixed at the same values as given previously corresponding to case A and case B. The colormaps in Fig.9-



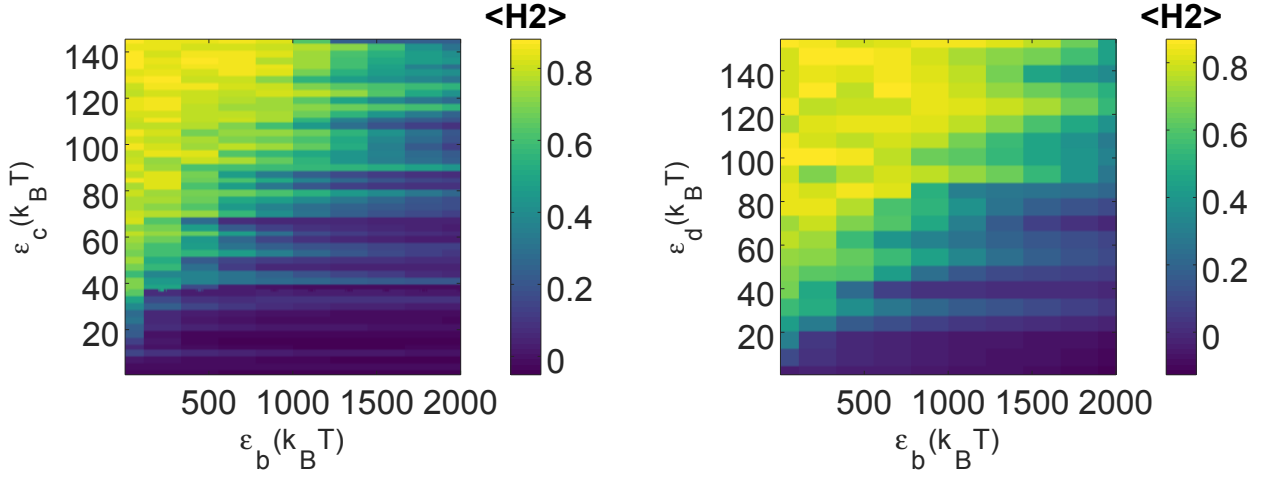


FIG. 9. Left colormap: At  $\kappa = 20k_B T/a^2$ , the state diagram shows the range of  $\epsilon_b$  and  $\epsilon_c$  for which one obtains helices. Right colormap: At  $\kappa = 10k_B T/a^2$ , the state diagram shows the range of  $\epsilon_b$  and  $\epsilon_d$  for which one obtains helices. The average  $\langle H2 \rangle$  was calculated from  $0.66\tau$ , to  $1.32\tau$ . This is because we expect the helix to have been formed by  $0.66\tau$ . When  $H2 < 0.2$ , one can hardly distinguish between a helical polymer and a semiflexible polymer with bends due to thermal fluctuations. The persistence length holds a linear relation with  $\epsilon_b$  such  $\ell_p = a\epsilon_b/k_B T$ , and the charge  $q$  per unit length  $a$  is  $q/a = \sqrt{4\pi\epsilon * \epsilon_c/a}$ . The dielectric constant of the medium is  $\epsilon$ .

indicate that for higher values of  $\epsilon_c$  (or  $\epsilon_d$ ), helices can be obtained for relatively higher values of  $\epsilon_b$  because the helix formation depends on the relative strengths of  $u_c$  (or  $u_d$ ) and  $u_b$ .

A polymer with relatively very high values of  $\epsilon_b$  is unable to form helices as formation of sharp kinks will be prevented by very high bending energies. Kinks, even if formed, will relax to form configurations which are stretched out resulting in lower values of  $H2$  and higher values of pitch (as discussed later). The colour map in the subfigure on the right of Fig.9 also shows that case B leads to formation of helices even with higher values of  $\epsilon_b$  as compared to that in Case A. This is because, the polymer with  $u_c$  (case A) would cause the polymer contour to stretch out more with relatively larger pitch during helix formation at times  $t < \tau$  due to longer range of  $1/r$  potential as compared to that of  $1/r^3$ . This results in lower values of  $H2$  when  $\epsilon_c$  is high as compared to a polymer with  $u_d$  potential with similar high values of  $\epsilon_d$ . Similar arguments were discussed previously when discussing the long time relaxation of the helices in Figs.6(b,d). So when comparing helix formation in case A with case B with relatively large values of  $\epsilon_c, \epsilon_d$  (say, with the choice  $\epsilon_c = \epsilon_d$ ),  $H2$  values will be lower in case A, as helix formation will be suppressed more in case A than in case B at identical high values of  $\epsilon_b$ .

We have already discussed how  $\epsilon_b$  is related to the persistence length. Similarly, we must express  $\epsilon_c$  in terms of line charge density of a polymer. We remind the reader that for case-A the Coulomb repulsion between two similarly charged monomers of charge  $q$  placed at a distance of  $a$  from each other, is equal to  $\epsilon_c$ . Therefore,  $(q^2/4\pi\epsilon a) = \epsilon_c$ , where  $\epsilon$  denotes the dielectric

constant. Hence,

$$q/a = \sqrt{4\pi\epsilon * \epsilon_c/a}. \quad (4)$$

As a reference, if the distance between monomers is  $a = 10nm$ , then at  $T = 300K$ ,  $\epsilon_c = 87.27k_B T$  corresponds to a charge of  $\approx 36e$  on each monomer  $10nm$  apart in water. This corresponds to a polymer chain having a charge density lower than the charge density of DNA. Bare DNA has around  $22e$  charge in a  $3.7 nm$  segment [44]. So such transient helical configurations can be seen in DNA or polymers with line-charge densities lower than that of the DNA, if they become charged from a neutral configuration.

What determines the pitch of the helix and how can we control it? The procedure for calculating the most frequently occurring pitch (in units of monomers) is detailed in the supplementary section. Once formed, the pitch of the helix increases with time as the helical structure gradually unwinds over time to decrease bending energy costs. To that end, we show the variation of the (most frequently occurring) pitch  $P$  versus time in Fig.10a for a chain length of  $N = 100$  monomers for a semiflexible polymer with  $u_c$  acting between the monomers. A polymer with large  $N$  is chosen so that the fourier transform calculation yields more accurate results (refer supplementary). The quantity  $P$  increases with increasing  $\epsilon_b$  (refer Fig.10b) as a higher value of  $\epsilon_b$  results in a higher energy cost associated with the local bends along the polymer chain. Thus a higher value of  $\epsilon_b$  gives rise to fewer loops along the chain, or a higher average value of the pitch. We did not observe any significant dependence of the pitch on  $\kappa$  and  $\epsilon_c$  (or  $\epsilon_d$ ). The corresponding data for  $P$

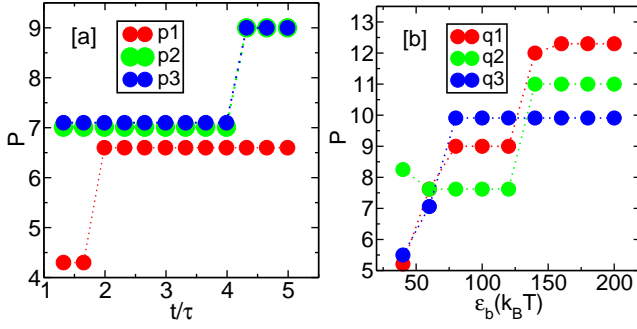


FIG. 10. (a) Plot of the (most frequently occurring) pitch  $P$  versus time for a chain of 100 monomers for  $\kappa = 20k_B T/a^2$ ,  $\epsilon_b = 10k_B T$  &  $\epsilon_c = 87.27k_B T$  (Case A) for 3 independent runs indicated by p1, p2 and p3. (b) At a fixed time  $t = \tau$ , we plot the (most frequently occurring) pitch  $P$  versus  $\epsilon_b$  for 3 independent runs q1, q2 and q3. The other parameters correspond to that of Case A. The figures corresponding to Case B is given in the supplementary.

(versus time and  $\epsilon_b$ ) with  $u_d$  acting between all monomer pairs (Case B) are given in the supplementary.

In Fig.10a we see that the quantity  $P$  is constant over some time before it abruptly shifts to a higher value. We explain how  $P$  is calculated to understand why that is the case. When we calculate the pitch, we take the Fourier transform of the quantity  $W$ , which is the dot product of bond vectors along the contour with a vector perpendicular to the axis of the helical polymer chain. Refer supplementary for the procedure of calculating  $P$  and also refer the figures which show the different values of the pitches obtained in the same helical configuration as it evolves with time. Thus, different segments of the chain form helical structures with slightly different values of the pitch. These in turn unwind at different rates. Hence there is more than one peak in the Fourier Spectrum of 'W' at any given instant of time. The monomer index corresponding to the peak with the highest amplitude at any given instant of time is denoted as  $P$ . Thus  $P$  represents the most frequently occurring pitch in the helical polymer chain. As the helical structure gradually unwinds segment by segment, the pitch corresponding to a particular segment increases and consequently the amplitude of the corresponding peak in the Fourier spectrum changes. However there is a change in the quantity  $P$  for the entire polymer chain, only when the position of the highest peak in the Fourier Spectrum of 'W' changes. This is evident from Fig.6b of the Supplementary where the Fourier spectrum shows two significant peaks at time  $t/\tau = 1$ . The amplitude of the peak corresponding to a pitch of 9 monomers, gradually increases with time, until at time  $t/\tau = 4.33$ , the peak corresponding to 9 monomers becomes the peak with the highest amplitude. It is only at this point that we register a change in the value of  $P$  of the helical polymer chain. Thus, the most frequently occurring pitch in the helical polymer chain or

$P$  therefore shows abrupt jumps in time.

In Fig.10b, where we show the dependence of  $P$  with  $\epsilon_b$ , we choose not to calculate the ensemble mean, since there are large differences in the values of  $P$  at a fixed instant of time corresponding to different runs. To illustrate this point we show three independent runs, which show considerable differences in the value of pitch, at the same time and for the same value of  $\epsilon_b$ . The difference in the values of  $P$  for independent runs arise due to the fact that initially the helix formation is triggered by the presence of thermal fluctuations.

As we saw earlier, that the formation of the helix depends on the strength of the Coulomb interaction  $\epsilon_c$  or on the value of  $\epsilon_d$ . The question is if the value of  $\epsilon_c$  in the model polymer chain increases gradually with time, i.e. a neutral semi-flexible chain gradually becomes charged (e.g. say, due to change in pH), does the polymer still form a helix if it starts out from a relatively straight configuration in the presence of thermal fluctuations? Moreover, can the helix formation occur in a recurring manner as a response to a time dependent periodic repulsive interaction?

To that end, we choose a significantly more rigid polymer such that the persistence length is much larger than the contour length of the polymer chain with  $N = 49$  monomers. We also choose a suitably higher charge density of the polymer chain. Moreover, we use a time dependent potential of the form  $u_c(t) = \epsilon_c(t)(a/r)$  where  $\epsilon_c(t) = \epsilon_c^0 * \cos^2(2\pi t/T_0)$  where we have chosen  $T_0 = 0.13\tau$ ,  $\epsilon_c^0 = 727.3k_B T$  and  $t$  denotes the simulation time. The values of  $\epsilon_b$  and  $\kappa$  was changed to  $300k_B T$  ( $\ell_p = 300a$ ) &  $1500k_B T/a^2$ , respectively, to have a stiffer chain. We observe that we obtain helices, in a recurring manner. The helices form, then dissolve away as  $\epsilon_c(t)$  becomes zero, such that the polymer becomes relatively straight in the thermal bath. The helical conformation forms again as the amplitude of the periodic forcing increases. To substantiate that we show  $H^2$  versus time  $t$  in Fig.11a for a chain of 49 monomers under the influence of  $u_c(t)$  and also for a chain of 49 monomers such that  $u_c = 0$ . We also show data for the same values of  $\kappa$  and  $\epsilon_b$  but  $u_d(t) = 769.34(a/r)^3 * \cos^2(2\pi t/T_0)$  in Fig.11b, where again we obtain helices in a recurring manner. The helices formed for these high values of  $\kappa$  and  $\epsilon_b$  dissolve away significantly faster as compared to that of cases A and B, and quickly return to a relatively straight conformation. This again emphasizes that the helix formation does not critically depend upon the straight line initial condition provided  $\ell_p$  is larger than the contour length; a factor of 6 in this case. Each time the polymer straightens up before reforming the helix, the configuration is slightly different due to the presence of  $k_B T$ .

Thus for the value of  $T_0$  chosen for this study, the helices can be made to form and dissolve away in a recurring, periodic fashion. The time scale  $\tau$  is decided by the value of the friction constant  $\zeta$ . Finally we want to put the relatively high value of  $\epsilon_c$  in perspective. If the distance between monomers in our calculation is taken

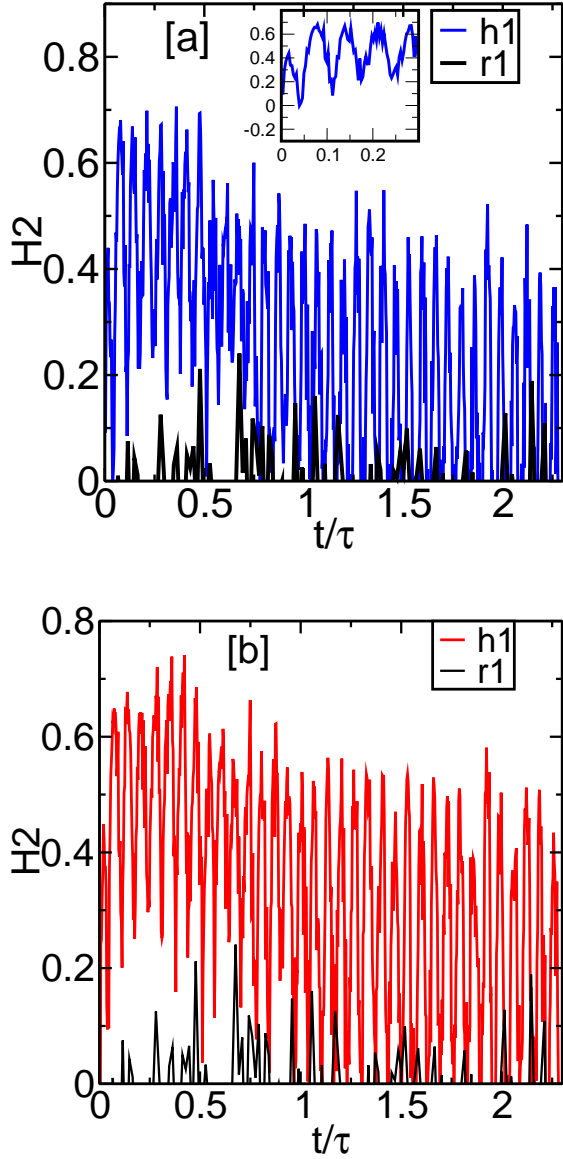


FIG. 11. Subfigure (a) shows  $H2$  versus time  $t$ , scaled by the relaxation time  $\tau$ , for a chain of 49 monomers with a time dependent  $U_c(t) = \epsilon_c^0 * (a/r) \cos^2(2\pi t/T_0)^2$  with  $T_0 = 0.13\tau$  over many cycles.  $H2$  varies periodically nearly in phase with the forcing. The inset shows that the periodicity is  $T_0/2$ . (b) Subfigure shows  $H2$  versus time for  $u_d(t)$  which has a similar time dependence as  $u_c(t)$ . We also give  $H2$  data for when  $u_c = 0$  and  $u_d = 0$ , denoted in the legend as  $r1$  for comparison of response.

as  $a = 10nm$ , then at  $T = 300K$ , the Coulomb energy  $\epsilon_c = 727k_B T$  used for the above study corresponds to a charge of  $\approx 108e$  on each monomer in water, i.e. a line charge density of  $\approx 11e$  per nm. As a reference, each base pair of DNA of size  $\approx 3.4\text{\AA}$  has a charge of  $\approx -2e$  at physiological pH [44]. Thus our choice of  $\epsilon_c$  in this case leads to a line charge density twice than that of DNA.

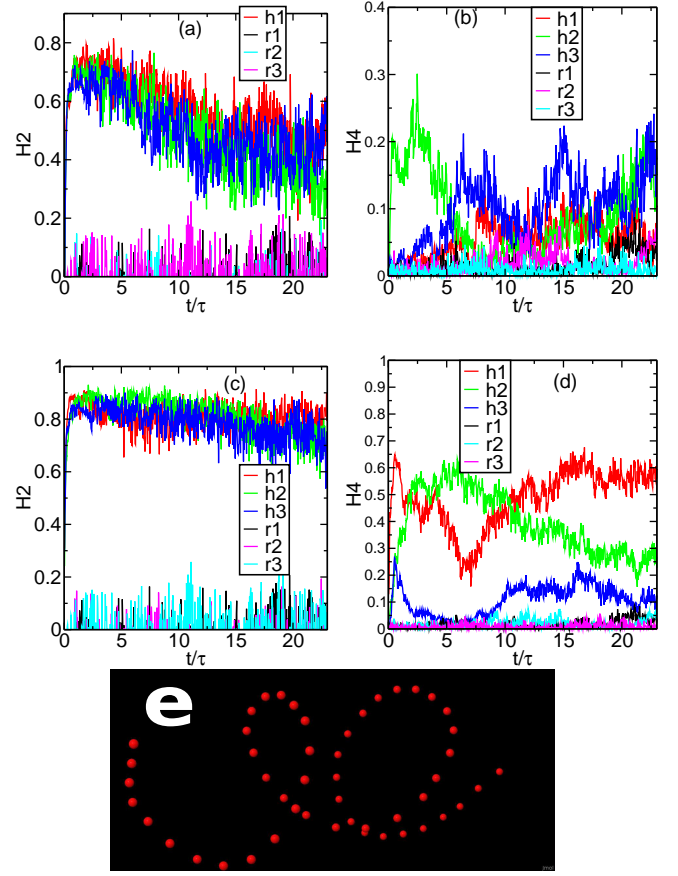


FIG. 12. Subplots (a) and (b) shows the evolution of order parameter  $H2$  and  $H4$  versus time for a semi-flexible polymer chain of 49 monomers with its end monomers fixed and forces due to potential  $u_c$  acting between all monomer pairs, with all parameters being identical to that of Case A. Subplots (c) and (d) shows the evolution of  $H2$  and  $H4$  versus time for a semiflexible polymer chain of 49 monomers with its end monomers fixed and forces due to potential  $u_d$  acting between all monomer pairs, with all parameters being identical to that of Case B. Subplot (e) shows the snapshot of a polymer chain of 49 monomers at  $t = 20\tau$ , with end monomers fixed and  $u_d$  acting between all monomer pairs and other parameters pertaining to that of Case B ( $H2 = 0.84$ ,  $H4 = 0.50$ ).

To explore whether the helical structure becomes more long-lived when the two ends of the polymer chain are grafted (tethered) on to two parallel surfaces, we do not update the positions of the end monomers of a polymer chain while observing the dynamics of the chain. The distance between the fixed monomers is equal to the contour length of the polymer chain (of 49 monomers) in the absence of charges. In this case the helical structures persist for a longer duration of time as compared to the helical structures resulting from a free standing polymer. This can be surmised from the data given in Fig.12. With  $u_c$  acting between the monomers, Figure 12a shows that there is a slight increase in the value of  $H2$  for a polymer chain at longer times (e.g. at time  $t = 20\tau$ ) as compared to a free standing polymer chain at similar times refer

Fig.2b. Moreover, Fig.12c shows that there is a significant increase in the value of  $H2$  at long times (at  $20\tau$ ) as compared to an free standing polymer chain with  $u_d$  acting between the monomer pairs at similar long times, refer Fig.2d. Thus we conclude that the tethering hinders the relaxation of transient helical structure by preventing it to stretch axially. The effects are more pronounced with the interaction potential  $u_d$ . A snapshot of the helical conformation of a polymer chain of 49 monomers with end monomers fixed and  $u_d$  acting between the monomer pairs has also been provided in Fig.12e.

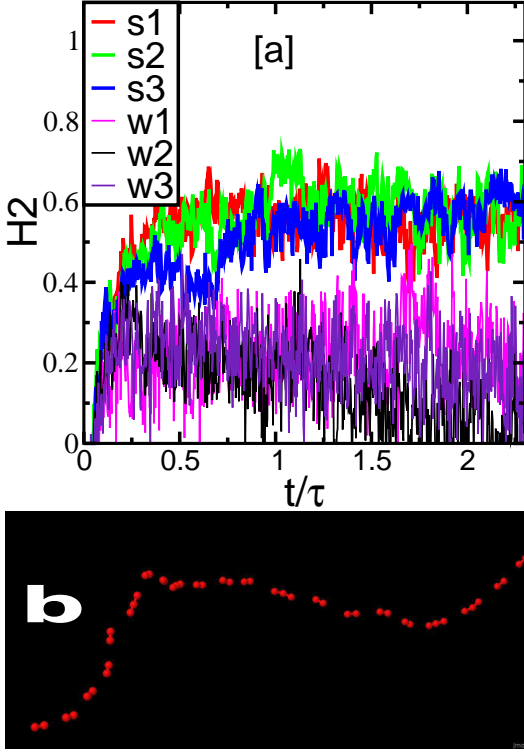


FIG. 13. Subplot (a) shows  $H2$  versus time for two different values of  $k_{int} = \epsilon_{lj}/\epsilon_c$  (where  $\epsilon_{lj}/4$  is the depth of the Lennard Jones potential) with three independent runs corresponding to each value. All parameters are identical to that of Case A. 's1', 's2' and 's3' denote three independent runs for  $k_{int} = 2.29$ , while 'w1', 'w2' and 'w3' denote three independent runs for  $k_{int} = 3.43$ . Subplot (b) shows the snapshot of the configuration of the polymer chain of 49 monomers for  $k_{int} = 3.43$  at  $t = 230\tau$ .

In our simulations so far we have implicitly assumed the solvent to be a good solvent. To investigate if the solvent quality affects helix formation, we present data for simulations with polymer in bad solvent conditions. To model bad solvent conditions, we apply an attractive Lennard Jones (LJ) interaction (of potential depth  $= \epsilon_{lj}/4$ ). This is used in conjunction with the repulsive Coulomb interaction  $u_c$  with all parameters pertaining to that of Case A to study transient helix formation. A polymer in a bad solvent would lead to a collapse of the polymer, where as the Coulomb repulsion would keep the

polymer in a stretched condition. We show that as long as strength of attractive interaction is relatively low as compared to the repulsive Coulomb interaction, we manage to obtain helices. If the ratio of the Lennard Jones interaction strength to the strength of the repulsive interaction i.e ( $k_{int} = \epsilon_{lj}/\epsilon_c$ ), is greater than a certain critical value, then the helix formation is prevented. For a polymer chain of 49 monomers with  $u_c$  ( $\epsilon_c = 87.27k_B T$ ) acting between all monomer pairs and other parameters kept identical to that of Case A, if  $k_{int}$  is lesser than  $k_{int} = 3.43$ , only then do we obtain helices. To substantiate the same, we have Fig.13 where we show  $H2$  values versus time for a polymer chain of 49 monomers with  $k_{int} = 2.29$  ('s1', 's2' and 's3' correspond to independent runs) while 'w1', 'w2' and 'w3' denote three independent runs with  $k_{int} = 3.43$ . We note that for all the three runs the value of  $H2$  is significantly greater for  $k_{int} = 2.29$ . For  $k_{int} = 3.43$  one obtains a long lived configuration with small clusters of monomers separated by stretched springs as shown in Fig.13b. A detailed study of the effect of unscreened Coulomb interaction and polymer collapse due to bad solvent conditions, and how the minimum value required for helix formation,  $k_{int}^c$ , depends on the chain length can be explored in a future study.

#### IV. DISCUSSIONS AND OUTLOOK

In conclusion, we demonstrate that spherically symmetric long ranged *repulsion* can give rise to transient helices in a semi-flexible polymer. This is a consequence of the long range of the interactions used which helps to radially spread out the sharp kinks that are formed at short times by the polymer chain due to a combination of thermal forces and repulsive interactions between monomers. Importantly, we have considered the charges on the polymer chains to be unscreened by counterions. Our model is minimal by design and therefore doesn't take into account atomistic chemical details of the monomers or the solvent particles. We find our findings non-intuitive a priori, because in previous studies emergent helices (in the absence of torsional potentials) are observed typically as a consequence of packing effects due to confinement or energy minimization due to short ranged attractive interactions in filaments, where sharp kinks are explicitly prevented.

The transient helix formation that we observe cannot be analyzed using geometric or a energy minimization calculation as the minimum (free) energy configuration in the presence of Coulomb potential  $u_c$  (or  $u_d$ ) is not a helix; it is a straight line configuration with deviations due to thermal fluctuations. However, a uncharged polymeric chain, which is slightly perturbed from a straight line initial condition or is in a bent configuration at  $T = 0$ , is put in conditions such that the charge on the monomer gets switched on at a time  $t = 0$ , it relaxes to equilibrium through a kinetically driven pathway where the intermediate stage is a helical configuration. This observation



remains true even if we start out with a stiff polymer in thermal equilibrium with a solvent bath. The same phenomenon happens even if the monomer charge increases gradually from zero as shown in Fig.11. Interestingly, we can get the helix to form in a recursive fashion as has been demonstrated in Fig.11 as the charge is gradually increased and then decreased back to zero in a periodic manner.

Since a free standing charged polymer chain tends to stretch out axially at long times, we can also use the charging and discharging of a (tethered) polymer chain to apply forces at the two surfaces to which the end monomers are kept attached. We obtain transient helices also on switching on a repulsive  $1/r^3$  potentials for a stiff polymer in a thermal bath as long as the persistence length is greater than the contour length of the polymer chain. Since the charge densities required to see the transient formation is very much realizable in the laboratory, we hope that our study will spur future experiments.

Our proposed mechanism can be possibly used to design helical springs for NEMs/MEMs devices at  $10nm-\mu$  length scales and using material of choice by arresting the relaxation process at a suitable time. As an example, we have shown that we obtain relatively long lived-helices by fixing both the ends of the chain and switching on the repulsive interactions between the monomers. In this case the helical structures persist for a longer duration of time as compared to the helical structures resulting from a free standing polymer, especially when we use  $1/r^3$  interaction potentials. Since the relaxation time of the polymer chain depends on the friction constant  $\zeta$ , a charged polymer can be made to relax slowly by placing it in a solvent of higher viscosity.

We thank K.Guruswamy and Bipul Biswas for useful discussions. We have used computer cluster obtained using DBT Grant BT/PR16542/BID/7/654/2016 to AC. AC acknowledges funding by DST Nanomission, India, the Thematic Unit Program (Grant No. SR/NM/TP-13/2016), MTR/2019/000078 and discussions in Statphys meetings in ICTS, Bangalore, India.

### Appendix A: Persistence length

If we have a semi-flexible polymer chain with just the harmonic spring interaction  $u_H$  and the potential  $u_b = \epsilon_b \cos \theta$  which introduces semi-flexibility along the

chain contour then, the energy required to bend a triplet of monomers of semi-flexible chain from its straight line configuration (such that  $\theta_0 = \pi$  and energy  $u_b = -\epsilon_b$ ) to a configuration with  $\theta < \pi$  is provided by the thermal energy. Therefore, if we equate the bending energy with the thermal energy and choose  $k_B T = 1$  as we use  $k_B T$  as the unit of energy:

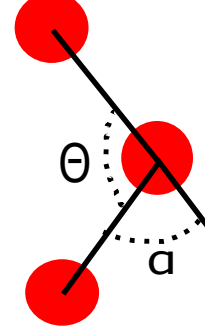


FIG. 14. A schematic diagram showing a triplet of monomers in red and defining the angle  $\theta$  and  $\alpha$  for the convenience of the reader.

$$\epsilon_b(\cos(\theta) - \cos(\pi)) \approx k_B T \quad (A1)$$

$$\equiv \cos \pi - \cos \theta = \frac{-1}{\epsilon'_b}. \quad (A2)$$

where,

$$\epsilon'_b = \epsilon_b / k_B T. \quad (A3)$$

If we define  $\alpha = (\pi - \theta)$ , then

$$-\cos \theta = \cos \alpha = (\epsilon'_b - 1)/\epsilon'_b \quad (A4)$$

For small values of  $\eta$ , one can write:

$$(1 - \frac{\alpha^2}{2}) = (\epsilon'_b - 1)/\epsilon'_b \equiv \alpha^2 = 2/\epsilon'_b \quad (A5)$$

From polymer physics [38], we know that for WLC (worm like chain) model, for the small angles of bends, the persistence length  $\ell_p$  is given by  $\ell_p = 2a/\alpha^2$ . Then using Eqn.3, the persistence length

$$\ell_p = a\epsilon_b / k_B T. \quad (A6)$$

[1] Jayanth R. Banavar, Trinh X. Hoang, Amos Maritan, Flavio Seno, and Antonio Trovato. Unified perspective on proteins: A physics approach. *Physical Review E*, 70(4), October 2004.

[2] S. J. Gerbode, J. R. Puzey, A. G. McCormick, and L. Mahadevan. How the cucumber tendril coils and overwinds. *Science*, 337(6098):1087–1091, August 2012.

- [3] Y. Forterre and J. Dumais. Generating helices in nature. *Science*, 333(6050):1715–1716, September 2011.
- [4] Amos Maritan, Cristian Micheletti, Antonio Trovato, and Jayanth R. Banavar. Optimal shapes of compact strings. *Nature*, 406(6793):287–290, July 2000.
- [5] B. Pokroy, S. H. Kang, L. Mahadevan, and J. Aizenberg. Self-organization of a mesoscale bristle into ordered, hierarchical helical assemblies. *Science*, 323(5911):237–240, January 2009.
- [6] Sid Ahmed Sabeur, Fatima Hamdache, and Friederike Schmid. Kinetically driven helix formation during the homopolymer collapse process. *Physical Review E*, 77(2), February 2008.
- [7] Huaping Li and Alkan Kabakçioğlu. Role of helicity in DNA hairpin folding dynamics. *Physical Review Letters*, 121(13), September 2018.
- [8] Daniel A. Vega, Andrey Milchev, Friederike Schmid, and Mariano Febbo. Anomalous slowdown of polymer detachment dynamics on carbon nanotubes. *Physical Review Letters*, 122(21), May 2019.
- [9] Y. Snir. Entropically driven helix formation. *Science*, 307(5712):1067–1067, February 2005.
- [10] Gaoshan Huang and Yongfeng Mei. Helices in micro-world: Materials, properties, and applications. *Journal of Materials*, 1(4):296–306, December 2015.
- [11] Pu Xian Gao, Wenjie Mai, and Zhong Lin Wang. Superelasticity and nanofracture mechanics of ZnO nanohelices. *Nano Letters*, 6(11):2536–2543, November 2006.
- [12] Xiang Yang Kong and Zhong Lin Wang. Spontaneous polarization-induced nanohelices, nanosprings, and nanorings of piezoelectric nanobelts. *Nano Letters*, 3(12):1625–1631, December 2003.
- [13] Soichiro Tottori, Li Zhang, Famin Qiu, Krzysztof K. Krawczyk, Alfredo Franco-Obregón, and Bradley J. Nelson. Magnetic helical micromachines: Fabrication, controlled swimming, and cargo transport. *Advanced Materials*, 24(6):811–816, January 2012.
- [14] Ambarish Ghosh and Peer Fischer. Controlled propulsion of artificial magnetic nanostructured propellers. *Nano Letters*, 9(6):2243–2245, June 2009.
- [15] Li Zhang, Jake J. Abbott, Lixin Dong, Kathrin E. Peyer, Bradley E. Kratochvil, Haixin Zhang, Christos Bergeles, and Bradley J. Nelson. Characterizing the swimming properties of artificial bacterial flagella. *Nano Letters*, 9(10):3663–3667, October 2009.
- [16] Li Zhang, Kathrin E. Peyer, and Bradley J. Nelson. Artificial bacterial flagella for micromanipulation. *Lab on a Chip*, 10(17):2203, 2010.
- [17] Yong Wang, Jun Xu, Yawen Wang, and Hongyu Chen. Emerging chirality in nanoscience. *Chem. Soc. Rev.*, 42(7):2930–2962, 2013.
- [18] W. Wang, K. Yang, J. Gaillard, P.R. Bandaru, and A. M. Rao. Rational synthesis of helically coiled carbon nanowires and nanotubes through the use of tin and indium catalysts. *Advanced Materials*, 20(1):179–182, January 2008.
- [19] Hai-Feng Zhang, Chong-Min Wang, and Lai-Sheng Wang. Helical crystalline SiC/SiO<sub>2</sub> core-shell nanowires. *Nano Letters*, 2(9):941–944, September 2002.
- [20] Hai-Feng Zhang, Chong-Min Wang, Edgar C. Buck, and Lai-Sheng Wang. Synthesis, characterization, and manipulation of helical SiO<sub>2</sub> nanosprings. *Nano Letters*, 3(5):577–580, May 2003.
- [21] Lichun Liu, Sang-Hoon Yoo, Sang A. Lee, and Sungho Park. Wet-chemical synthesis of palladium nanosprings. *Nano Letters*, 11(9):3979–3982, September 2011.
- [22] K. Robbie, D. J. Broer, and M. J. Brett. Chiral nematic order in liquid crystals imposed by an engineered inorganic nanostructure. *Nature*, 399(6738):764–766, June 1999.
- [23] D. C. Rapaport. Molecular dynamics simulation of polymer helix formation using rigid-link methods. *Physical Review E*, 66(1), July 2002.
- [24] Debasish Chaudhuri and Bela M. Mulder. Spontaneous helicity of a polymer with side loops confined to a cylinder. *Physical Review Letters*, 108(26), June 2012.
- [25] Sunita Sanwaria, Sajan Singh, Andriy Horechyy, Petr Formanek, Manfred Stamm, Rajiv Srivastava, and Bhanu Nandan. Multifunctional core-shell polymer-inorganic hybrid nanofibers prepared via block copolymer self-assembly. *RSC Advances*, 5(109):89861–89868, 2015.
- [26] Tatjana Škrbić, Jayanth R. Banavar, and Achille Giacometti. Chain stiffness bridges conventional polymer and bio-molecular phases. *The Journal of Chemical Physics*, 151(17):174901, November 2019.
- [27] B. J. Haupt, T. J. Senden, and E. M. Sevick. AFM evidence of rayleigh instability in single polymer chains. *Langmuir*, 18(6):2174–2182, March 2002.
- [28] F Oosterhelt, M Rief, and H E Gaub. Single molecule force spectroscopy by AFM indicates helical structure of poly(ethylene-glycol) in water. *New Journal of Physics*, 1:6–6, January 1999.
- [29] Luke J. Kirwan, Georg Papastavrou, Michal Borkovec, and Sven H. Behrens. Imaging the coil-to-globule conformational transition of a weak polyelectrolyte by tuning the polyelectrolyte charge density. *Nano Letters*, 4(1):149–152, January 2004.
- [30] A. Katchalsky, J. Mazur, and P. Spitnik. SECTION II: Polybase properties of polyvinylamine. *Journal of Polymer Science*, 23(104):513–532, February 1957.
- [31] G. Kocak, C. Tuncer, and V. Büttin. pH-responsive polymers. *Polymer Chemistry*, 8(1):144–176, 2017.
- [32] Karthika Suresh and Guruswamy Kumaraswamy. Effect of electrostatic interactions on structure and mechanical properties of ice templated colloid-polymer composites. *Journal of Physics D: Applied Physics*, 52(21):214002, March 2019.
- [33] Guruswamy Kumaraswamy, Karthika Suresh, Hisayama, Madivala G. Basavaraj, and Dillip K. Satapathy. Ice templated nanocomposites containing rod-like hematite particles: Interplay between particle anisotropy and particle-matrix interactions. *Journal of Applied Physics*, 128(3):034702, July 2020.
- [34] Miklós Orbán, Krisztina Kurin-Csörgei, and Irving R. Epstein. pH-regulated chemical oscillators. *Accounts of Chemical Research*, 48(3):593–601, February 2015.
- [35] Benjamin J. T. Dodd and Joel M. Kralj. Live cell imaging reveals pH oscillations in *saccharomyces cerevisiae* during metabolic transitions. *Scientific Reports*, 7(1), October 2017.
- [36] Bipul Biswas, Raj Kumar Manna, Abhrajit Laskar, P. B. Sunil Kumar, Ronjoy Adhikari, and Guruswamy Kumaraswamy. Linking catalyst-coated isotropic colloids into “active” flexible chains enhances their diffusivity. *ACS Nano*, 11(10):10025–10031, September 2017.

- [37] Guruswamy Kumaraswamy, Bipul Biswas, and Chandan Kumar Choudhury. Colloidal assembly by ice templating. *Faraday Discussions*, 186:61–76, 2016.
- [38] Michael Rubinstein and Ralph H Colby. *Polymer Physics*. Oxford University Press, 2003.
- [39] J. P Kemp and J. Z. Y Chen. Folding dynamics of the helical structure observed in a minimal model. *Europhysics Letters (EPL)*, 59(5):721–727, September 2002.
- [40] Gerald S. Manning. The persistence length of DNA is reached from the persistence length of its null isomer through an internal electrostatic stretching force. *Biophysical Journal*, 91(10):3607–3616, November 2006.
- [41] Emmanuel Trizac and Tongye Shen. Bending stiff charged polymers: The electrostatic persistence length. *EPL (Europhysics Letters)*, 116(1):18007, October 2016.
- [42] Andrey V. Dobrynin. Electrostatic persistence length of semiflexible and flexible polyelectrolytes. *Macromolecules*, 38(22):9304–9314, November 2005.
- [43] Hao Li and T. A. Witten. Fluctuations and persistence length of charged flexible polymers. *Macromolecules*, 28(17):5921–5927, August 1995.
- [44] R. Milo and R. Phillips. *Cell Biology by the Numbers*. CRC Press, 2015.